CRYSTAL
GROWTH
& DESIGN
2008
VOL. 8, NO. 2
587–591

One-Dimensional Double Helical Structure and 4-Fold Type [2 + 2] Interpenetration of Diamondoid Networks with Helical Fashion

Ho Yong Lee,[†] Jaejoon Park,[‡] Myoung Soo Lah,*[,‡] and Jong-In Hong*[,†]

Department of Chemistry, College of Natural Sciences, Seoul National University, Seoul 151-747, and Department of Chemistry and Applied Chemistry, College of Science and Technology, Hanyang University, Ansan, Kyunggi-Do 426-791, Korea

Received August 1, 2007; Revised Manuscript Received October 29, 2007

ABSTRACT: We have prepared unique homochiral structures by the self-assembly of a modified amino acid derivative (terephthaloylmonoalanine, *L*-TMA) with metal ions such as Zn(II) and Cd(II). An *L*-TMA ligand and Zn(II) ions formed a left-handed, homochiral, double helical chain. However, while *L*-TMA and Cd(II) ions topologically formed a diamondoid Cd-*L*-TMA network with 4-fold type [2 + 2] interpenetration, Cd-*L*-TMA can be morphologically considered as a three-dimensional network of left-handed, double helices. The double helical structure of Zn-*L*-TMA originated from the self-assembly of individual helical chains by hydrogen bonds and $\pi-\pi$ interactions, whereas the double helical structures of Cd-*L*-TMA were observed in an interpenetrating diamondoid net.

Introduction

An enormous research effort has been directed at inducing chirality at the supramolecular level. Recent reports about homochiral coordination polymers[1] suggest the possibility of applications to enantioselective separation,[1a] catalytic processes[1a,h] and magneto-optical processes.[1e] Therefore, a lot of effort has been devoted to the development of new homochiral coordination polymers. These are usually based on the self-assembly between metal ions and chiral bridging ligands.[2] The chirality of the building block affects the chirality of the resulting structure itself, as well as its folding and interpenetration patterns. Examination of the interpenetration pattern of the chiral coordination polymers is very important, as different chiral structures can be created through interpenetration.

Among interpenetration nets, three-dimensional (3D), diamondoid-related structures are common and have been widely studied.[3] Diamondoid-related nets are usually composed of linear ligands with a connecting tetrahedral node. However, diamondoid nets using chiral ligands are less common. The common interpenetration mode of the diamondoid net has been widely studied and is well-established. The interpenetration pattern with an unusual mode[3,4] remains difficult to predict or fully explain. Many factors, such as hydrogen bonds and $\pi-\pi$ and lipophilic interactions, exert a complicated influence over interpenetration of the diamondoid net. Herein, we report the unique homochiral structures obtained by self-assembly using an amino acid derivative (terephthaloylmonoalanine, *L*-TMA) with transition metal ions [Zn(II) and Cd(II)].[5] An *L*-TMA ligand and Zn(II) ions form a left-handed, homochiral, double helical chain. A schematic representation of the Zn-*L*-TMA and Cd-*L*-TMA structures is presented in Scheme 1.

L-TMA and Cd(II) ions form a diamondoid network with 4-fold type [2 + 2] interpenetration in a double helical fashion. The two structures show a similar packing pattern with respect to the double helical structure. Examination of the structural relationship between Zn-*L*-TMA and Cd-*L*-TMA will further elucidate the interpenetration pattern of the diamondoid net.

Scheme 1. Schematic Representation of Zn-*L*-TMA and Cd-*L*-TMA Structures

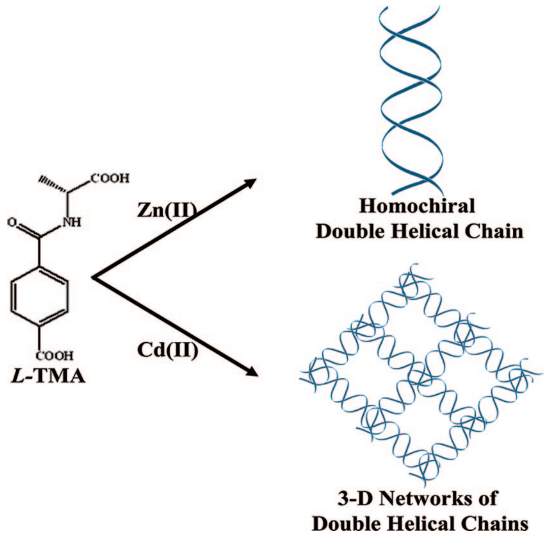

Experimental Section

Synthesis of the *L*-TMA Ligand. Oxalyl chloride in methylene chloride (2 M solution, 3 mL) was added to a stirred solution of terephthalic acid monomethyl ester (1.0 g, 5.5 mmol) in distilled methylene chloride (10 mL) under nitrogen. After this solution was stirred at room temperature for 3 h, the reaction mixture was evaporated in vacuo. A solution of the reaction mixture in methylene chloride (20 mL) at 0 °C under nitrogen was added dropwise to a solution of *L*-alanine methyl ester HCl (770 mg, 1 equiv, 5.5 mmol) in methylene chloride (50 mL) and TEA (2.5 equiv). After the resulting solution was stirred for an additional 3 h at room temperature, the residue was partitioned into water and methylene chloride and extracted three times with methylene chloride. The organic layer was washed with water and brine, dried with $MgSO_4$, and evaporated in vacuo. The residue was dissolved in methylene chloride (20 mL), and a white solid was precipitated by adding hexane. The desired ligand (*L*-TMA) was formed by hydrolysis and acidification. Recrystallization in water produced a colorless crystal (940 mg, 72% overall yield).

^{1}H NMR (DMSO-d_6, 300 MHz): 13.14 (broad s, 2H), 8.88 (d, 1H, $J = 7.26$ Hz), 8.03 (d, 2H, $J = 7.59$ Hz), 7.98 (d, 2H, $J = 8.55$ Hz),

---

* To whom correspondence should be addressed. Fax: (+82)2-889-1568. E-mail: (J.-I.H.) jihong@snu.ac.kr and (M.S.L.) mslah@hanyang.ac.kr.

[†] Seoul National University.

[‡] Hanyang University.

10.1021/cg7007232 CCC: $40.75 © 2008 American Chemical Society
Published on Web 01/23/2008

Table 1. Selected Crystallographic Data for Zn-*L*-TMA and Cd-*L*-TMA

complex	Zn-*L*-TMA	Cd-*L*-TMA
formula	$C_{11}H_{17}NO_9Zn$	$C_{88}H_{146.5}Cd_8N_8O_{77.5}$
formula weight (g M^{-1})	372.63	3455.83
temperature (K)	173(2)	173(2)
crystal system	triclinic	monoclinic
space group	$P1$	$P2_1$
a (Å)	8.8575(10)	16.704(1)
b (Å)	9.0761(11)	14.0024(9)
c (Å)	9.9599(12)	26.822(2)
α (°)	85.761(2)	90
β (°)	81.076(2)	91.165(1)
γ (°)	71.338(2)	90
volume (Å^3)	749.16(15)	6272.3(7)
Z	2	2
D_{calcd} (kg/m^3)	1.652×10^{-6}	1.830×10^{-6}
absorption coefficient (mm^{-1})	1.684	1.442
reflections collected	3929	39589
independent reflections	3154 [R(int) = 0.0151]	27880 [R(int) = 0.0220]
data/restraints/parameters	3154/19/450	27880/1/1850
goodness-of-fit on F^2	1.125	1.029
final R indices [$I > 2\sigma(I)$]	$R1 = 0.0273$, $wR2 = 0.0742$	$R1 = 0.0304$, $wR2 = 0.0717$
R indices (all data)	$R1 = 0.0283$, $wR2 = 0.0746$	$R1 = 0.0337$, $wR2 = 0.0733$
absolute structure parameter	0.031(13)	−0.02(1)
largest diff. peak and hole (e Å^{-3})	0.651 and −0.398	0.932 and −0.836

4.46 (m, 1H), 1.41 (d, 3H, $J = 7.35$ Hz). ^{13}C NMR (DMSO-d_6, 75 MHz): 174.44, 176.23, 138.17, 133.62, 129.89, 128.10, 48.70, 17.29. HRMS (ESI): calcd for $C_{11}H_{11}NO_5$ (M+), 237.0637; found, 237.0637.

Preparation of Zn-*L*-TMA Complex. After the slow mixing of *L*-TMA (20 mg, 0.065 mmol) in water (2 mL) deprotonated with 2 equiv of NaOH and $Zn(NO_3)_2 \cdot 6H_2O$ (25 mg, 1 equiv) in EtOH (2 mL), a vial containing the filtrate was left at room temperature to evaporate. After 7 days, colorless crystals suitable for single-crystal X-ray diffraction (XRD) analysis were obtained from the vial wall. Elemental analysis $[C_{22}H_{18}N_2O_{10}Zn_2 \cdot (H_2O)_6]$: calcd: C, 37.26; H, 4.26; N, 3.95. Found: C, 37.20; H, 4.39; N, 3.97.

Preparation of Cd-*L*-TMA Complex. After the slow mixing of *L*-TMA (20 mg, 0.065 mmol) in water (2 mL) deprotonated with 2 equiv of NaOH and $Cd(NO_3)_2 \cdot 4H_2O$ (25 mg, 1 equiv) in EtOH (2 mL), a vial containing the filtrate was left at room temperature to evaporate. After 7 days, we were able to obtain colorless crystals from the vial wall suitable for single-crystal XRD analysis. Elemental analysis $[C_{88}H_{88}N_8O_{40}Cd_8(H_2O)_{20}] \cdot 15H_2O$: calcd: C, 30.84; H, 4.65; N, 3.27. Found: C, 30.81; H, 4.70; N, 3.25.

Crystallographic Data Collection and Structure Refinement. Both crystals coated with paratone oil were mounted on a glass capillary. The diffraction data were measured at 173 K with Mo Kα radiation (λ = 0.71073 Å) on a Bruker SMART CCD equipped with a graphite crystal, incident-beam monochromator. The structures were elucidated by direct methods and refined by full-matrix, least-squares calculations with the SHELXTL-PLUS software package (Sheldrick, G. M., Brukers Analytical X-Ray Division, Madison, WI, 1997).

X-ray Crystallographic Analysis for Zn-*L*-TMA. All nonhydrogen atoms were refined anisotropically. All hydroxyl hydrogen atoms were found in difference Fourier maps and refined with an assigned isotropic displacement coefficient of U(H) = 1.5 U (OH) and a restraint bond distance of 0.82 Å. The remaining hydrogen atoms were assigned isotropic displacement coefficients of U(H) = 1.2 U (C, N) or 1.5 U (C-methyl), and their coordinates were allowed to ride on their respective atoms. Crystallographic details are given in Table 1.

X-ray Crystallographic Analysis for Cd-*L*-TMA. At least 18 solvent–water sites were identified, some of which were statically disordered. All of the nonhydrogen atoms were refined anisotropically. The hydrogen atoms were assigned isotropic displacement coefficients of U(H) = 1.2 U (C, N) or 1.5 U (OH, C-methyl), and their coordinates were allowed to ride on their respective atoms. Crystallographic details are given in Table 1.

Results and Discussion

Two complexes (Zn-*L*-TMA and Cd-*L*-TMA) were formed by the same procedure. After slow mixing of deprotonated *L*-TMA by treatment with 2 equiv of NaOH in water and metal ions $[Zn(NO_3)_2 \cdot 6H_2O$ and $Cd(NO_3)_2 \cdot 4H_2O]$ in EtOH, a clear solution obtained by filtration was left at room temperature for evaporation of the volatiles. After 7 days, colorless crystals were obtained in the vial wall suitable for single-crystal XRD analysis.

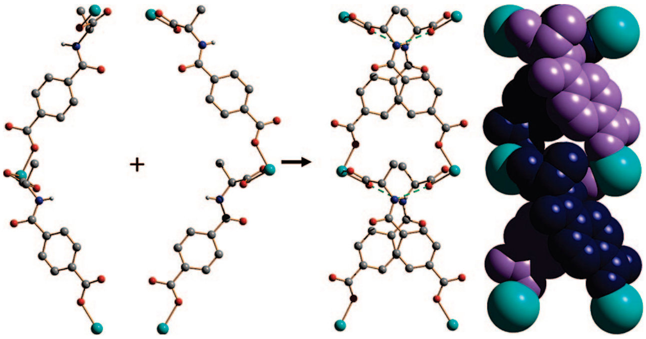

Figure 1. Formation of the Zn-*L*-TMA double helical structure. Ball and stick model (left): C (gray), O (red), N (blue), and Zn (bluish green). All hydrogen atoms except for amide hydrogens are omitted for clarity. Hydrogen bonds are represented by green dashed lines. CPK representation of Zn-*L*-TMA (right): Ligands of each helical chain are represented with the same colors except Zn(II) ions for clarity.

In the case of Zn(II) ions and the *L*-TMA complex (Zn-*L*-TMA), two *L*-TMA ligands and two Zn ions exist in the asymmetric unit. Zn1 of the Zn-*L*-TMA has a trigonal bipyramidal geometry by coordination of two carboxylate oxygen atoms [Zn1−O1, 2.116(4); Zn1−O7, 2.124(4) Å, syn-monodentate mode] and three water molecules. Another zinc ion (Zn2 of Zn-*L*-TMA) adopts an octahedral geometry due to the coordination of the syn-carboxylate oxygen [Zn2−O10, 2.075(4) Å], an asymmetric chelating carboxylate [Zn2−O4, 2.140(4); Zn2−O5, 2.280(5) Å], and three water molecules. Each resulting one-dimensional (1D) helical chain of the Zn-*L*-TMA is twisted around another in a left-handed manner, even though *L*-alanine derivatives are used. The two 1D helical chains are self-assembled into double helices through hydrogen bonds and $\pi-\pi$ interactions in a tilted mode (Figure 1). Amide NH protons are hydrogen-bonded with the carboxylate of the adjacent helical chain [N−H···O, d(D−H) = 0.88; d(H···A) = 2.05, 2.03 Å; and angle(DHA) = 160.2, 164.3°]. The pitch of the individual helix is 21.562(2) Å, and each turn comprises two Zn(II) ions and *L*-TMA ligands.

Table 2. Selected Bond Lengths (Å) and Angles (deg) for Cd-*L*-TMA[a]

Cd(1A)−O(4G)#1	2.261(3)	Cd(2B)−O(1F)	2.272(3)
Cd(1A)−O(1A)	2.272(3)	Cd(2B)−O(1E)	2.275(3)
Cd(1A)−O(5E)#2	2.307(3)	Cd(2B)−O(4A)	2.383(3)
Cd(1A)−O(2D)#3	2.335(3)	Cd(2B)−O(4B)	2.405(3)
Cd(1A)−O(1D)#3	2.500(3)	Cd(2B)−O(5B)	2.473(3)
Cd(1A)−O(4E)#2	2.531(2)	Cd(2B)−O(5A)	2.486(3)
Cd(3C)−O(4H)#4	2.252(3)	Cd(4D)−O(1G)	2.274(3)
Cd(3C)−O(1B)	2.285(3)	Cd(4D)−O(2H)	2.325(3)
Cd(3C)−O(2C)	2.297(3)	Cd(4D)−O(4C)	2.378(2)
Cd(3C)−O(5F)#5	2.304(3)	Cd(4D)−O(4D)	2.398(2)
Cd(3C)−O(4F)#5	2.580(2)	Cd(4D)−O(5C)	2.456(2)
Cd(3C)−O(1C)	2.608(3)	Cd(4D)−O(5D)	2.476(2)
Cd(5A)−O(4A)	2.354(2)	Cd(6B)−O(4B)	2.327(3)
Cd(7C)−O(4C)	2.396(2)	Cd(8C)−O(4D)	2.334(2)
O(4G)#1−Cd(1A)−O(1A)	84.75(10)	O(1F)−Cd(2B)−O(1E)	167.83(12)
O(4G)#1−Cd(1A)−O(5E)#2	172.52(9)	O(1F)−Cd(2B)−O(4A)	86.85(9)
O(1A)−Cd(1A)−O(5E)#2	92.79(10)	O(1E)−Cd(2B)−O(4A)	95.48(10)
O(4G)#1−Cd(1A)−O(2D)#3	95.13(11)	O(1F)−Cd(2B)−O(4B)	96.59(10)
O(1A)−Cd(1A)−O(2D)#3	178.80(10)	O(1E)−Cd(2B)−O(4B)	86.03(10)
O(5E)#2−Cd(1A)−O(2D)#3	87.19(10)	O(4A)−Cd(2B)−O(4B)	156.55(9)
O(4G)#1−Cd(1A)−O(1D)#3	87.11(9)	O(1F)−Cd(2B)−O(5B)	91.14(9)
O(1A)−Cd(1A)−O(1D)#3	124.83(10)	O(1E)−Cd(2B)−O(5B)	80.84(9)
O(5E)#2−Cd(1A)−O(1D)#3	88.53(9)	O(4A)−Cd(2B)−O(5B)	149.85(8)
O(2D)#3−Cd(1A)−O(1D)#3	53.97(9)	O(4B)−Cd(2B)−O(5B)	53.51(8)
O(4G)#1−Cd(1A)−O(4E)#2	133.56(9)	O(1F)−Cd(2B)−O(5A)	81.18(9)
O(1A)−Cd(1A)−O(4E)#2	93.73(9)	O(1E)−Cd(2B)−O(5A)	90.57(10)
O(5E)#2−Cd(1A)−O(4E)#2	53.57(9)	O(4A)−Cd(2B)−O(5A)	53.59(8)
O(2D)#3−Cd(1A)−O(4E)#2	87.22(9)	O(4B)−Cd(2B)−O(5A)	149.85(8)
O(1D)#3−Cd(1A)−O(4E)#2	128.59(9)	O(5B)−Cd(2B)−O(5A)	96.37(9)
O(4H)#4−Cd(3C)−O(1B)	90.83(10)	O(1G)−Cd(4D)−O(2H)	166.29(10)
O(4H)#4−Cd(3C)−O(2C)	92.14(10)	O(1G)−Cd(4D)−O(4C)	89.44(9)
O(1B)−Cd(3C)−O(2C)	176.99(10)	O(2H)−Cd(4D)−O(4C)	94.81(9)
O(4H)#4−Cd(3C)−O(5F)#5	172.67(9)	O(1G)−Cd(4D)−O(4D)	94.66(9)
O(1B)−Cd(3C)−O(5F)#5	92.36(10)	O(2H)−Cd(4D)−O(4D)	87.39(9)
O(2C)−Cd(3C)−O(5F)#5	84.64(10)	O(4C)−Cd(4D)−O(4D)	153.28(9)
O(4H)#4−Cd(3C)−O(4F)#5	133.50(9)	O(1G)−Cd(4D)−O(5C)	82.33(9)
O(1B)−Cd(3C)−O(4F)#5	88.84(9)	O(2H)−Cd(4D)−O(5C)	89.56(9)
O(2C)−Cd(3C)−O(4F)#5	89.46(8)	O(4C)−Cd(4D)−O(5C)	54.36(8)
O(5F)#5−Cd(3C)−O(4F)#5	53.21(9)	O(4D)−Cd(4D)−O(5C)	152.36(8)
O(4H)#4−Cd(3C)−O(1C)	86.35(9)	O(1G)−Cd(4D)−O(5D)	89.18(9)
O(1B)−Cd(3C)−O(1C)	126.80(9)	O(2H)−Cd(4D)−O(5D)	81.10(9)
O(2C)−Cd(3C)−O(1C)	53.00(9)	O(4C)−Cd(4D)−O(5D)	152.93(8)
O(5F)#5−Cd(3C)−O(1C)	86.46(9)	O(4D)−Cd(4D)−O(5D)	53.70(8)
O(4F)#5−Cd(3C)−O(1C)	129.00(8)	O(5C)−Cd(4D)−O(5D)	98.69(9)

[a] Symmetry transformations used to generate equivalent atoms: #1, $x - 1$, $y + 1$, $z + 1$; #2, $x - 1$, $y - 1$, z; #3, x, y, $z + 1$; #4, $x + 1$, $y + 1$, z; #5, $x + 1$, $y - 1$, z; #6, x, y, $z - 1$; #7, $x - 1$, $y + 1$, z; and #8, $x + 1$, $y - 1$, $z - 1$.

In the case of packing of the individual double helices, the coordinating water molecules are involved in the interconnection of the double helices via the hydrogen bond with the amide carbonyl group of the adjacent double helix.

Cd-*L*-TMA crystallizes in the chiral monoclinic space group $P2_1$. Two kinds of Cd(II) ions exist in the asymmetric unit of Cd-*L*-TMA (Figure 2). One class of Cd(II) ions (labeled as Cd1A, Cd2B, Cd3C, and Cd4D) binds four carboxylates, which act as a tetrahedral node in combination with the flexibility of the *L*-TMA ligand. Each Cd(II) ion adopts a distorted, octahedral geometry. The *L*-TMA ligands bridge two Cd(II) centers through their syn-monodentate carboxylate oxygen atoms and chelating carboxylate groups. Another class of Cd(II) ions (labeled as Cd5A, Cd6B, Cd7C, and Cd8C) is simply coordinated to carboxylates in a trans type, monodentate manner with no direct participation in the construction of a diamondoid network connectivity. These Cd(II) ions bind carboxylates to balance the overall charge of the diamondoid net. Five water molecules are coordinated to Cd(II) ions in adopting an octahedral geometry. Selected bond lengths and angles are listed in Table 2.

The diamondoid framework contains nanosized, distorted adamantanoid cages. The average separation of the adjacent Cd−Cd is 13.657 Å. A single cage is illustrated in Figure 3.

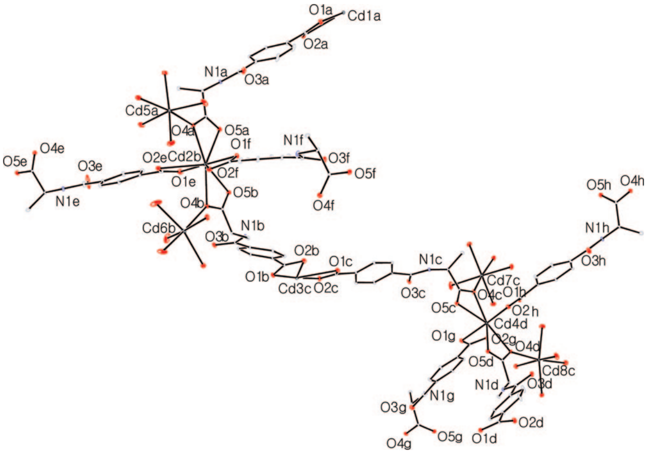

Figure 2. Asymmetric unit of Cd-*L*-TMA. Only the cadmium metals and the heteroatoms in the ligands are labeled. All of the hydrogen atoms are omitted for clarity.

Cd-*L*-TMA is a 4-fold, interpenetrating diamondoid network with guest water molecules and with an interpenetration mode that differs from the usually observed mode in such networks. In typical 4-fold diamondoid networks, the nodes of the independent nets are aligned and equally spaced along ideal

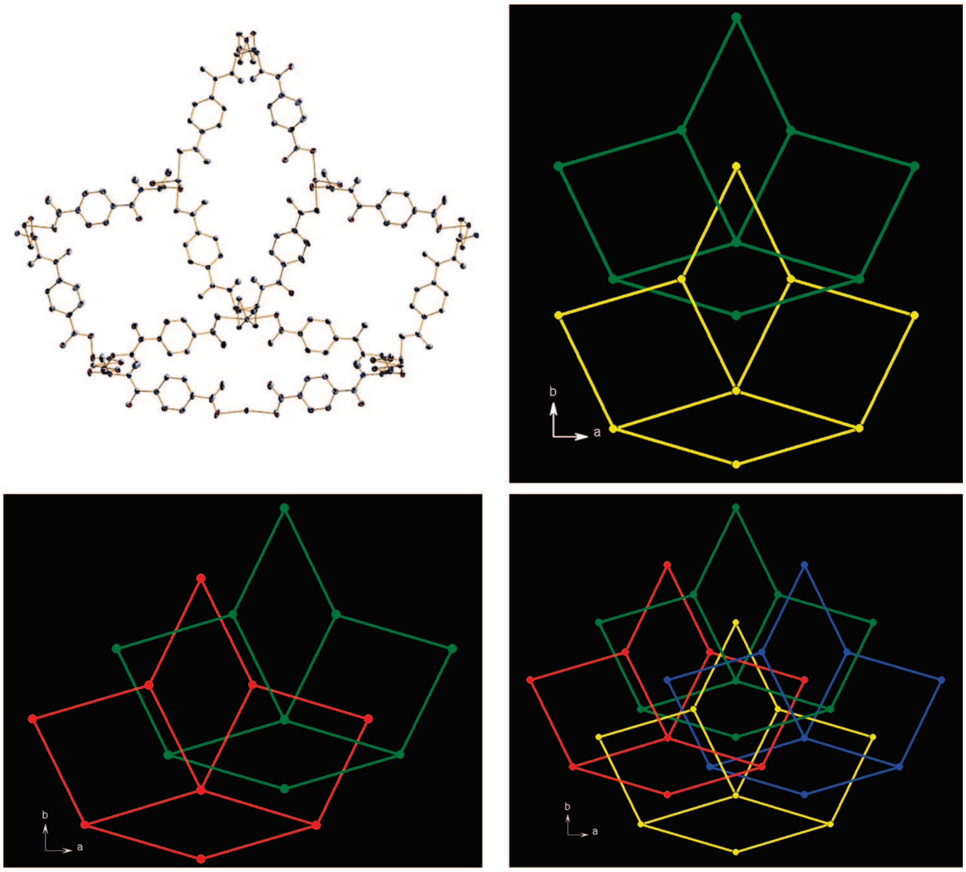

Figure 3. Adamantanoid cage (upper left). Schematic representation of the interpenetration pattern of green and yellow nets (upper right). Schematic representation of the interpenetration pattern of green and red nets (bottom left). Schematic representation of the overall [2 + 2] interpenetrating mode of diamondoid networks (bottom right). Hydrogen atoms and simply coordinating Cd(II) ions (Cd5A, Cd6B, Cd7C, and Cd8C) are omitted for clarity.

2-fold axes. However, in the case of Cd-*L*-TMA, interpenetrating nets of green−blue are rotationally equivalent with green−red net interpenetration, while green−blue and red−yellow nets are translationally equivalent. The interpenetration between green−blue and red−yellow nets results in a new, green−yellow, interpenetration pattern. Therefore, the overall interpenetration can be described as a twin-set, 2-fold net. Therefore, this unusual 4-fold interpenetration is regarded as a [2 + 2] interpenetrating diamondoid system.[4a]

In a typical interpenetrating diamondoid net, there is no $\pi-\pi$ interaction and no hydrogen bonds between two adamantanoid cages. However, the two nets investigated here are stabilized by hydrogen bonds between coordinating water molecules to Cd(II) ions, guest water molecules, amide groups, and carboxylate oxygens in a complex manner. In addition, three sides of the two interpenetrating adamantanoid cages are strongly joined via $\pi-\pi$ interactions and hydrogen bonds, generating infinite double helices.

As illustrated in Figure 4, the double helix resulting from this unusual interpenetration shows a very similar folding pattern to that of Zn-*L*-TMA. Amide NH protons are hydrogen-bonded with the carboxylates of the interpenetrating net. The helical pitch of the Cd-*L*-TMA double helix is 21.79 Å, which is slightly longer than that of Zn-*L*-TMA. Interpenetration of the diamondoid net induces a simple helical chain, packing pattern.

The overall 4-fold-type [2 + 2] interpenetrating mode, illustrated in Figure 5, is composed of left-handed, double helical chains, which originate from the interpenetration of the diamondoid nets. However, Cd-*L*-TMA can topologically be considered as a 3D network of left-handed double helices, which

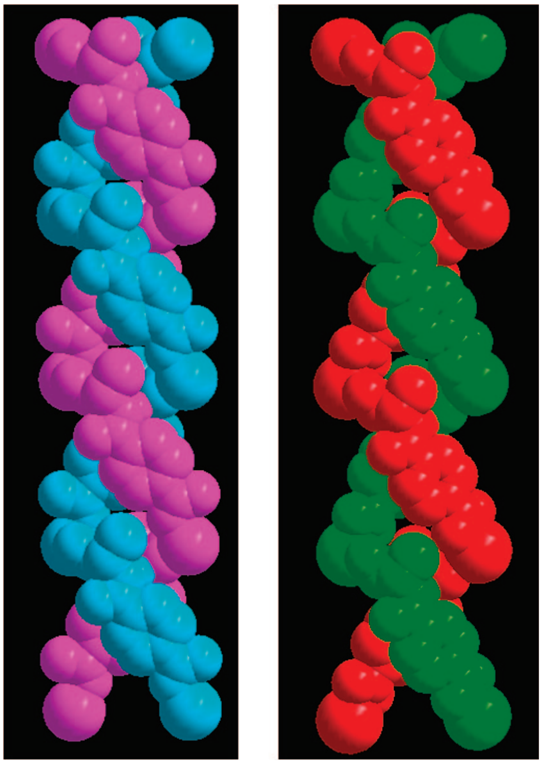

Figure 4. Zn-*L*-TMA double helix (left). One helical chain is indicated in pink, and the other is indicated in sky blue. The double helix resulted from unusual interpenetration of Cd-*L*-TMA (right). One helical chain is indicated in red, and the other is indicated in green.

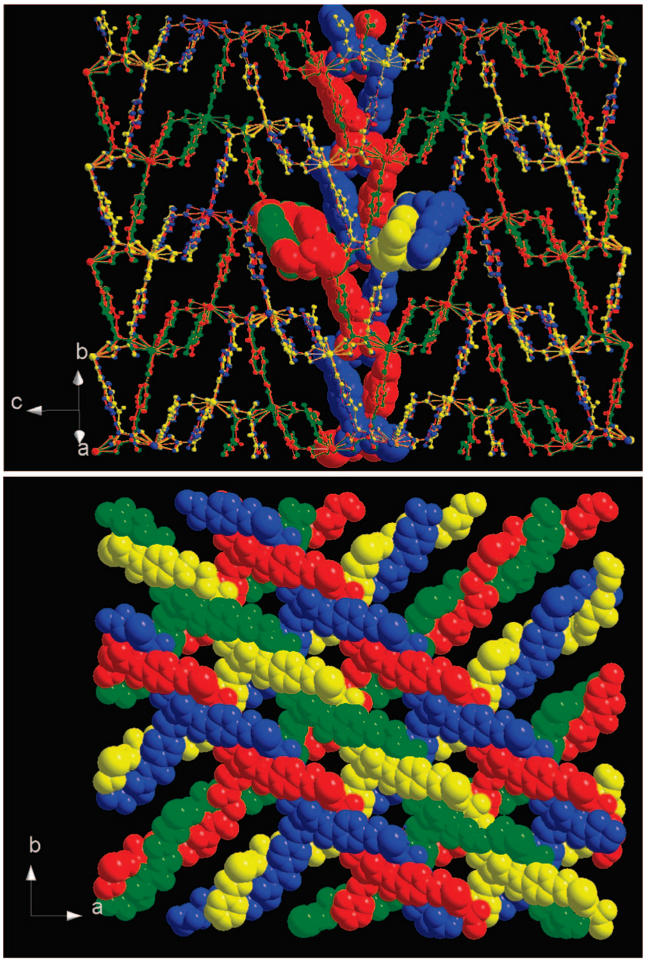

Figure 5. Four-fold [2 + 2] interpenetrating networks (top). Three crossing double helices are represented by the CPK mode. Partial view of the crossing double helices (bottom). The four nets are represented with different colors (blue, green, red, and yellow). Hydrogen atoms, guest water molecules, and simply coordinating Cd(II) ions (Cd5A, Cd6B, Cd7C, and Cd8C) are omitted for clarity.

are perpendicularly connected by Cd(II) ions. Therefore, the resulting interpenetrating structure can be regarded as a double helix network.

Conclusion

In conclusion, we have demonstrated the preparation of two unique, homochiral, coordination polymer structures. An *L*-TMA ligand derived from a natural amino acid demonstrated an excellent ability to form homochiral coordination polymers with two transition metal ions: Zn(II) and Cd(II). The Zn-*L*-TMA crystal structure was a double helical chain assembled by hydrogen bonds and $\pi-\pi$ interactions. Cd-*L*-TMA crystallized as a 4-fold-type [2 + 2], interpenetrating diamondoid network. The helical folding pattern of the Zn-*L*-TMA was observed in the interpenetrating diamondoid net of the Cd-*L*-TMA. The present study results promise to increase our understanding of the interpenetration of the diamondoid net based on a chiral bridging ligand, through a comparison of the Zn-*L*-TMA and Cd-*L*-TMA structures.

Acknowledgment. Support for this work through a grant from the MOCIE (Grant 10024945) is gratefully acknowledged. H.Y.L. thanks the Ministry of Education for the award of a BK 21 fellowship. M.S.L. also acknowledges the financial support of KOSEF (R01-2005-000-10490-0).

Supporting Information Available: CIF files of structures. This material is available free of charge via the Internet at http://pubs.acs.org.

References

(1) (a) Kesanli, B.; Lin, W. *Coord. Chem. Rev.* **2003**, *246*, 305–326, and references therein. (b) Anokhina, E. V.; Jacobson, A. J. *J. Am. Chem. Soc.* **2004**, *126*, 3044–3045. (c) Shi, X.; Zhu, G.; Qiu, S.; Huang, K.; Yu, J.; Xu, R. *Angew. Chem., Int. Ed.* **2004**, *43*, 6482. (d) Seitz, M.; Kaiser, A.; Stempfhuber, S.; Zabel, M.; Reiser, O. *J. Am. Chem. Soc.* **2004**, *126*, 11426–11427. (e) Imai, H.; Inoue, K.; Kikuchi, K.; Yoshida, Y.; Ito, M.; Sunahara, T.; Onaka, S. *Angew. Chem., Int. Ed.* **2004**, *43*, 5618–5621. (f) Noord, A. D. C.; Kampf, J. W.; Pecoraro, V. L. *Angew. Chem., Int. Ed.* **2002**, *41*, 4668–4670. (g) Sreennivasulu, B.; Vittal, J. *Angew. Chem., Int. Ed.* **2004**, *43*, 5769–5772. (h) Wu, C.-D.; Hu, A.; Zhang, L.; Lin, W. *J. Am. Chem. Soc.* **2005**, *127*, 8940–8941. (i) Wu, C.-D.; Lin, W. *Inorg. Chem.* **2005**, *44*, 1178–1180. (j) Jiang, H.; Lin, W. *J. Am. Chem. Soc.* **2003**, *125*, 8084–8085.

(2) Chiral coordination polymers from achiral ligands: Ezuhara, T.; Endo, K.; Aoyama, Y. *J. Am. Chem. Soc.* **1999**, *121*, 3279–3283.

(3) Reviews: (a) Batten, S. R.; Robson, R. *Angew. Chem., Int. Ed.* **1998**, *37*, 1460−1494. (b) Batten, S. R. *Curr. Opin. Solid State Mater. Sci.* **2001**, *5*, 107–114. (c) Batten, S. R. *CrystEngComm.* **2001**, *3*, 67–72. (d) Yaghi, O. M.; Li, H.; Davis, C.; Richardson, D.; Groy, R. L. *Acc. Chem. Res.* **1998**, *31*, 474–484. (e) Evans, O. R.; Lin, W. *Acc. Chem. Res.* **2002**, *35*, 511–522. Recent examples of the diamondoid networks: (f) Li, X.; Cao, R.; Sun, D.; Bi, W.; Wang, Y.; Li, X.; Hong, M. *Cryst. Growth. Des.* **2004**, *4*, 775−780. (g) Madalan, A. M.; Kravtsov, V. C.; Simonov, Y. A.; Voronkova, V.; Korobchenko, L.; Avarvari, N.; Andruh, M. *Cryst. Growth Des.* **2005**, *5*, 45–47. (h) Du, M.; Bu, X.-H.; Guo, Y.-M.; Liu, H. *Inorg. Chem.* **2002**, *41*, 4904–4908. (i) Kumar, D. K.; Jose, D. A.; Das, A.; Dastidar, P. *Inorg. Chem.* **2005**, *44*, 6933–6935. (j) Liang, K.; Zheng, H.; Song, Y.; Lappert, M. F.; Li, Y.; Xin, X.; Huang, Z.; Chen, J.; Lu, S. *Angew. Chem., Int. Ed.* **2004**, *43*, 5776–5779. (k) Liu, Y.-H.; Wu, H.-C.; Lin, H.-M.; Hou, W.-H.; Lu, K.-L. *Chem. Commun.* **2003**, 60–61.

(4) (a) Unusual interpenetrating diamondoid networks: Carlucci, L.; Ciani, G.; Proserpio, D. M.; Rizzato, S. *Chem. Eur. J.* **2002**, *8*, 1520–1526. (b) Batten, S. R.; Harris, A. R.; Jensen, P.; Murray, K. S.; Ziebell, A. *J. Chem. Soc., Dalton Trans.* **2000**, 3829–3835. (c) Kim, H.; Suh, M. P. *Inorg. Chem.* **2005**, *44*, 810–812.

(5) Interpenetrating networks using pseudopeptidic ligand and transition metal ions: Kostakis, G. E.; Casella, L.; Hadjiliadis, N.; Monzani, E.; Kourkoumelis, N.; Plakatouras, J. C. *Chem. Commun.* **2005**, 3859–3861.

CG7007232